THE GERONTOLOGICAL SOCIETY OF AMERICA®

Journals of Gerontology: Biological Sciences
cite as: *J Gerontol A Biol Sci Med Sci*, 2019, Vol. 74, No. 5, 625–633
doi:10.1093/gerona/gly175
Advance Access publication July 31, 2018

OXFORD

Original Article

Chronic Resveratrol Treatment Reduces the Pro-angiogenic Effect of Human Fibroblast "Senescent-Associated Secretory Phenotype" on Endothelial Colony-Forming Cells: The Role of IL8

Beatrice Menicacci, PhD student,[1,2,*] Francesca Margheri, PhD,[1,*] Anna Laurenzana, PhD,[1] Anastasia Chillà, PhD,[1] Mario Del Rosso, MSc,[1] Lisa Giovannelli, PhD,[3] Gabriella Fibbi, PhD,[1] and Alessandra Mocali, PhD[1]

[1]Department of Experimental and Clinical Biomedical Science "Mario Serio", Section of Experimental Pathology and Oncology, University of Florence. [2]Department of Medical Biotechnologies, University of Siena. [3]Department NeuroFarBa, Section of Pharmacology and Toxicology, University of Florence, Italy.

*These authors contributed equally to this work.

Address correspondence to: Alessandra Mocali, PhD, Department of Experimental and Clinical Biomedical Science "Mario Serio", Section of Experimental Pathology and Oncology, University of Florence, Viale G.B. Morgagni 50, 50134 Florence, Italy. E-mail: amocali@unifi.it

Received: March 21, 2018; Editorial Decision Date: July 24, 2018

Decision Editor: David Le Couteur, MBBS, FRACP, PhD

Abstract

Senescent cells are characterized by an increased secretion of inflammatory and growth factors, known as the "senescence-associated secretory phenotype" (SASP), producing a pro-tumoral and pro-angiogenic microenvironment. This work proposes chronic resveratrol treatment (5 μM for 5 weeks, termed R5) of senescent MRC5 fibroblasts as a mean to mimic and target the angiogenic trait of stromal fibroblast SASP. Senescent fibroblast conditioned medium (CM sen) was effective in enhancing the angiogenic properties of endothelial colony-forming cells (ECFCs), that is, invasive activity and capillary morphogenesis capability in vitro, that were significantly reduced when conditioned media were collected after resveratrol pretreatment (CM senR5). The attenuation of ECFC angiogenic phenotype induced by CM senR5 was accompanied by reduced protein levels of epidermal growth factor and urokinase plasminogen activator receptors (EGFR, uPAR), and by a related decreased activation of receptor-tyrosine-kinase signaling pathways. IL8 levels were found reduced in CM senR5 compared to CM sen, with the associated reduction of IL8–CXCR2 binding in ECFCs. IL8-subtraction mitigated the pro-angiogenic features of CM sen and the associated intracellular signaling in ECFCs, indicating a prominent role of IL8 in the pro-angiogenic effects of CM sen. IL8 modulation is an important mechanism underlying the antiangiogenic activity of resveratrol on MRC5 SASP.

Keywords: Resveratrol, Cellular senescence, Endothelial cell, Microenvironment, IL8

Fibroblast senescence creates a cancer-favoring microenvironment through release of secreted factors that define the so-called "senescence-associated secretory phenotype" (SASP) (1). An element of complexity in tumor progression is represented by the inventory of "normal" cells that have been shown to favor some of the classic hallmarks of cancer and that are referred to as "tumor microenvironment." Among the cells of the tumor microenvironment, senescent fibroblasts show features resembling those of cancer-associated fibroblasts (2,3), reported to promote proliferation and invasion of cancer cells with several mechanisms (4). Cancer progression depends heavily on the development of a vascular network whereby new vessels ensure adequate supply of oxygen, nutrients, and growth factors, fostering at the same time cancer growth and dissemination. Tumor cells produce several angiogenic factors that stimulate the "classical" endothelial sprouting angiogenesis, which is

performed by mature endothelial cells of the host. In particular, the property to induce a sustained angiogenesis is established as one of the main hallmarks of cancer, whose control is holding promises following the use of antiangiogenic agents as a complementary therapy of many human tumors (5). IL8 is an important component of SASP (6), which may contribute to reinforce autocrine senescent cell-growth arrest (7) and has been found to be highly increased in media conditioned by senescent endothelial cell cultures (8). SASP IL8 exerts paracrine actions, activating endothelial cells and inducing migration behavior (9,10). Indeed IL8, together with IL6, has been reported to confer a more aggressive phenotype to breast cancer cells exposed to a senescent microenvironment (11). It is now widely accepted that endothelium-dependent vessels in the tumor also develop by the process of vasculogenesis, in which endothelial colony-forming cells (ECFCs) are recruited within the tumor from the circulation. In addition, tumor cells actively participate in neovascularization through (i) vasculogenic mimicry, (ii) trans-differentiation of cancer stem cells to tumor endothelial cells, and (iii) vascular co-option, resulting into mosaic vessels formed by tumor and endothelial cells (12). Along the natural history of a tumor, the endothelium-dependent vessels, deriving from both angiogenesis and vasculogenesis, will progressively substitute vascular mimicry, trans-differentiation, and cancer cell co-option, to become the principal route of blood supply to malignant cells (13). Like many types of cancers, cellular senescence is related to aging and here we show a data set indicating that senescent fibroblast SASP creates a vasculogenic environment that promotes vessel formation by endothelial progenitor cells.

The stilbene resveratrol is a non-flavonoid polyphenol endowed with many health-promoting activities that have been much studied. Among these, it is able to counteract the aging process in vivo, protecting both cognitive and motor functions, preserving tissues acting as a diet restriction mimetic, and improving skeletal muscle function through mitochondrial biogenesis, in long term–treated rodents (14–16). In vitro, we have shown in long term–treated human fibroblasts its ability to ameliorate senescence-associated dysfunctions, such as reduced cell proliferation and adhesion capacity, to reduce hallmarks of senescence such as cellular and nuclear enlargement, β-galactosidase activity, and nuclear DNA damage, and to mitigate the SASP (17,18). This last result prompted us to investigate whether the treatment with resveratrol could effectively modify tumor microenvironment, and indeed we recently demonstrated that the reduction of soluble signaling factors and proteases secreted by senescent fibroblasts upon resveratrol treatment was associated with reduced pro-tumor effects on melanoma cell proliferation and invasiveness, and with reduced expression of epithelial-to-mesenchymal transition markers related to malignant features (19). Thus, these data indicate that resveratrol can indirectly modify pro-tumor signaling in cancer cells by acting on the senescent stromal cell phenotype. It is well known that resveratrol is also able to interact directly with different tumor cells, exerting antiproliferative and pro-apoptotic effects, as well as counteracting epithelial-to-mesenchymal transition (20), presumably through different molecular mechanisms, among which are the antioxidant activity, the reduction of NFkB activation and its cytokine signaling cascade, the interference with cell cycle components, and with the balance of pro-and antiapoptotic factors (21). Furthermore, resveratrol reduces macrophage activation and migration and modulates T lymphocytes and natural killer cells (22). In addition, the antiangiogenic direct effect of resveratrol has been reported (23), mainly ascribed to its antioxidant properties (24). All in all, this polyphenol appears to be able to act on different stroma components to inhibit all the stages of tumorigenesis, a feature that can be useful both in tumor therapy and prevention (25).

The aim of the present work was to evaluate the ability of resveratrol to modify also the angiogenic component of the tumor microenvironment. Here we provide evidence that the long-term treatment of senescent fibroblasts with resveratrol does reduce the vasculogenic activity of MRC5 fibroblast SASP. We also demonstrate that resveratrol-treated senescent fibroblasts have a reduced ability to promote new vessel formation in vitro by the endothelial progenitor cells, compared to untreated senescent cells, and that this feature can be mainly ascribed to the reduction of secreted IL8.

Materials and Methods

Cell Cultures

MRC5 cell lines are normal human fetal lung fibroblasts purchased from National Institute of Aging Cell Repository (Coriell Institute). MRC5 were cultured in high-glucose (4,500 mg/L) Dulbecco's Modified Eagle's Medium (Euroclone) supplemented with 10% fetal bovine serum (FBS, Sigma-Aldrich), 2 mM l-glutamine, 100 units/mL penicillin, and 100 µg/mL streptomycin (Sigma-Aldrich) at 37°C in 5% CO_2 humidified atmosphere, and propagated at confluence by trypsinization. ECFCs were isolated from >50 mL human umbilical cord blood of healthy newborns, as described previously (26) after maternal informed consent and in compliance with Italian legislation, and analyzed for the expression of surface antigens (CD45, CD34, CD31, CD105, ULEX, vWF, KDR, and uPAR) by flow cytometry (26). ECFCs were selected as $CD45^-$, $CD34^+$, $CD31^+$, $CD105^+$, $ULEX^+$, vWF^+, and KDR^+ cells and were grown in EGM-2 culture medium (Lonza), supplemented with 10% FBS onto gelatin-coated dishes.

MRC5 Senescence Characterization and Resveratrol Treatment

The experiments with MRC5 fibroblasts were conducted on pre-senescent cultures, defined as having undergone population doubling level (PDL) more than 45, and after 5 weeks propagation in culture with or without 5 µM final resveratrol (Sigma-Aldrich) concentration, these cells became senescent as described previously (17). At the end of treatment, senescent control and resveratrol-treated MRC5 cultures were referred to as sen and senR5, respectively. Low PDL (<30) MRC5 fibroblasts were also propagated in culture and referred to as young.

During treatment, control and R5-treated fibroblasts were analyzed for their proliferative activity by viable (Trypan-blue negative) cell counting; in parallel, senescence-associated β-galactosidase staining and p16 protein levels were determined, as previously reported (27), at t = 0 and at t = 30 days. For senescence-associated β-galactosidase staining, cultures were examined under phase-contrast microscopy at ×200 magnification.

TUNEL Assay

TdT-mediated dUTP Nick-End Labeling (TUNEL) assay was carried out using the Dead End Fluorometric TUNEL system (Promega) according to the manufacturer's instructions. In brief, young, sen, and senR5 MRC5 were seeded on the coverslips, fixed in 4% paraformaldehyde in phosphate-buffered saline (PBS), permeabilized in 0.2% Triton X-100 in PBS, and incubated with the TUNEL reaction mixture containing TdT and fluorescein-labeled dUTP for 1 hour at 37°C. Nuclei were counterstained with 4′,6-diamidino-2-phenyindole (DAPI). DNase I (10 U/mL in PBS) treatment was performed on sen MRC5 cells as positive control. The apoptotic cells were revealed using confocal laser scanning microscope (Nikon).

Preparation of Conditioned Media

EBM plus 2% FBS was added, after washing with PBS, to MRC5 cell cultures in a ratio of 1 mL/100,000 cells. Conditioned media (MRC5

CM) were collected after 24 hours incubation from untreated young, sen, and senR5-treated fibroblasts, and centrifuged at 1,500 rpm for 5 minutes. These conditioned media were referred to as CM young, CM sen, and CM senR5, respectively. The unconditioned medium also contained 2% FBS and was indicated as EBM.

All media were stored at −80 °C until use.

IL8 Expression: Real Time Polymerase Chain Reaction on MRC5 Cells and ELISA Detection in Conditioned Media

Total RNA extraction was performed using TRIzol reagent (Invitrogen). RNA was reverse transcribed with iScript cDNA Synthesis Kit using random primers. mRNA expression of IL8 and 18S-rRNA gene was assayed by real time polymerase chain reaction (PCR) using the following primers (IDT, TemaRicerca).

IL-8: forward 5′-ATAAAGACATACTCCAAACCTTTCCAC-3′
reverse 5′-AAGCTTTACAATAATTTCTGTGTTGGC-3′
18S-rRNA: forward, 5′-CCAGTAAGTGCGGGTCATAAG-3′
reverse, 5′-GCCTCACATAA-CCATCCAATC-3′

Quantitative real time PCR was performed with an Applied Biosystem 7500 Fast RT PCR System (Applied Biosystem) using a SYBR Green–based detection with the default PCR setting: 40 cycles of 95°C for 15 seconds and of 60°C for 60 seconds. The "Delta-delta method" was used for comparing relative gene expression results using 18 seconds as the housekeeping gene. Data were normalized to results obtained in young MRC5 (assumed as value 1) and expressed as means ± standard deviation (*SD*) of three experiments.

To remove IL8 from conditioned medium, CM sen was incubated with an irrelevant IgG (reported as CM sen + I IgG) or 2 µg/mL of anti-IL8 antibody (Santa Cruz Biotech Biotechnologies; reported as CM sen + anti-IL8 Ab) for 30 minutes at room temperature with constant rotation. Then, both CMs were added with 1.5 mg of Dynabeads Protein G (Life Technologies), and incubated for 10 minutes at room temperature with constant rotation. The conditioned media were subsequently separated from Dynabeads Protein G, recovered, and used immediately for IL8 detection and ECFC incubation. Mini TMB ELISA Development Kit (PeproTech, DBA) was used for IL-8 detection according to the manufacturer's instructions. Each sample was tested in duplicate and three independent experiments were performed.

ECFC Treatment With MRC5 CM

ECFCs (12×10^4 per well) were seeded in six-well plates; once grown to approximately 80% confluency, cells were incubated overnight with 1 mL unconditioned EBM, or different conditioned media, and subsequently recovered by trypsinization for Western blot analyses or for invasion and capillary morphogenesis assays. The experimental design is depicted in Supplementary Figure 3 and described in the following paragraphs.

Invasion Assays in Boyden Chambers

Analyses were performed in Boyden chambers, with wells separated by 8-µm-pore size polycarbonate filters coated with Matrigel (50 µg/filter). In chemoinvasion experiments, subconfluent ECFCs were recovered by trypsinization, counted, then 2×10^4 cells were suspended in 200 µL EBM plus 2% FBS and placed in upper well, while in the lower one 200 µL of either MRC5 conditioned media or unconditioned medium (used as reference) were placed. In spontaneous invasion experiments, ECFCs cultures were preincubated overnight with EBM or MRC5 CM. Then, cells from each incubation group were detached and counted as earlier, then resuspended in 200 µL of the same conditioned media in which were incubated overnight and placed in the upper well of Boyden chambers. Fresh EBM plus 2% FBS was placed in the lower well. In both types of experiments, invasion was performed for 6 hours at 37°C in 5% CO_2, then filters were recovered and fixed in methanol. Non-invading cells on the upper surface of the filter were removed with a cotton swab whereas invasive cells adherent on the lower filter surface were stained and counted using a light microscope.

For chemoinvasion assay, results were expressed as the percentage of cells migrated toward MRC5 CM compared to those migrated toward EBM. For spontaneous invasion activity determination, results were reported as the percentage of ECFCs migrated after preincubation with MRC5 CM compared to those migrated after preincubation with EBM.

Wound-Healing Assay

ECFCs (12×10^4 per well) were seeded in six-well plates and grown to confluency. The standard culture medium was then substituted with different CMs or standard EBM, and a wound was produced in each well with a 20 µL micropipette tip. Microphotographs of the wound were taken at 0, 6, and 18 hours. Images were analyzed with the Image J MRI Wound healing software and reported as the percentage of the residual wound compared to initial wound area.

Capillary Morphogenesis

In vitro capillary morphogenesis was performed as described (26,28) in tissue culture wells coated with Matrigel (BD Biosciences). ECFCs, after overnight pretreatment with EBM or MRC5 CM, were resuspended (18×10^3/well in 96 well plates) for 6 hours in the same incubation media at 37°C in 5% CO_2. Results were quantified at the end of experiment with Angiogenesis Analyzer tool of Image J software, measuring the number of junctions, branches and tubules, total length, and total tubules length. Six to nine photographic fields from three plates were analyzed for each point.

Western Blot Analyses

Cell aliquots of MRC5 and ECFCs were collected at the end of the respective treatments and lysed in RIPA buffer (25 mM Tris–HCl pH 7.6, 150 mM NaCl, 1% NP-40, 1% sodium deoxycholate, 0.1% sodium dodecyl sulfate) with 1% protease inhibitor Cocktail (Sigma-Aldrich) and disrupted by sonication (Microson XL-2000, Misonix). Lysates were clarified by centrifugation and supernatant collected and stored at −20°C. Protein content was measured trough Bradford assay. Protein aliquots (25–40 µg), were separated by 12% sodium dodecyl sulfate –polyacrylamide gel electrophoresis (NuPAGE, Novex; Invitrogen), transferred to nitrocellulose membranes (Millipore), blocked in 5% skim milk, and incubated overnight with the specific primary antibodies: rabbit anti-p16 (Santa Cruz Biotech), mouse anti-tubulin (Sigma-Aldrich), mouse anti-CXCR2 (Santa Cruz Biotech), mouse anti-uPAR (Santa Cruz Biotech) that recognizes the full-length uPAR, rabbit anti-phospho-ERK (p42/p44, Santa Cruz Biotech), rabbit anti-EGFR (Santa Cruz Biotech), rabbit anti-phospho AKT (Cell Signaling), rabbit anti-phospho-S6 (Cell Signaling), and mouse anti-phospo-STAT3 (Santa Cruz Biotech) followed by the suitable HRP-conjugated secondary antibodies (Sigma-Aldrich). All the resulting immunocomplexes were visualized with an enhanced chemiluminescence ECL detection system (GE Healthcare) and quantified by ImageJ software (NIH).

FACS Analysis of Cell Surface CXCR2 Expression

30 × 10^4 ECFCs/well were seeded in six-well plates; once grown to approximately 80% confluency, cells were incubated overnight with unconditioned EBM plus 2% FBS, referred to as EBM, or with MRC5 CM (CM sen or CM senR5) and subsequently recovered by Accutase (Euroclone). IL8 receptor expression was assessed using anti-human CXCR2-phicorytrin conjugated mAbs (R&D Systems). Cells were incubated 20 minutes with the mAb on ice, washed twice in 1% FBS–PBS, and analyzed with a FACScan Cytometer (Beckman Coulter). Each analysis was performed on at least 10,000 events.

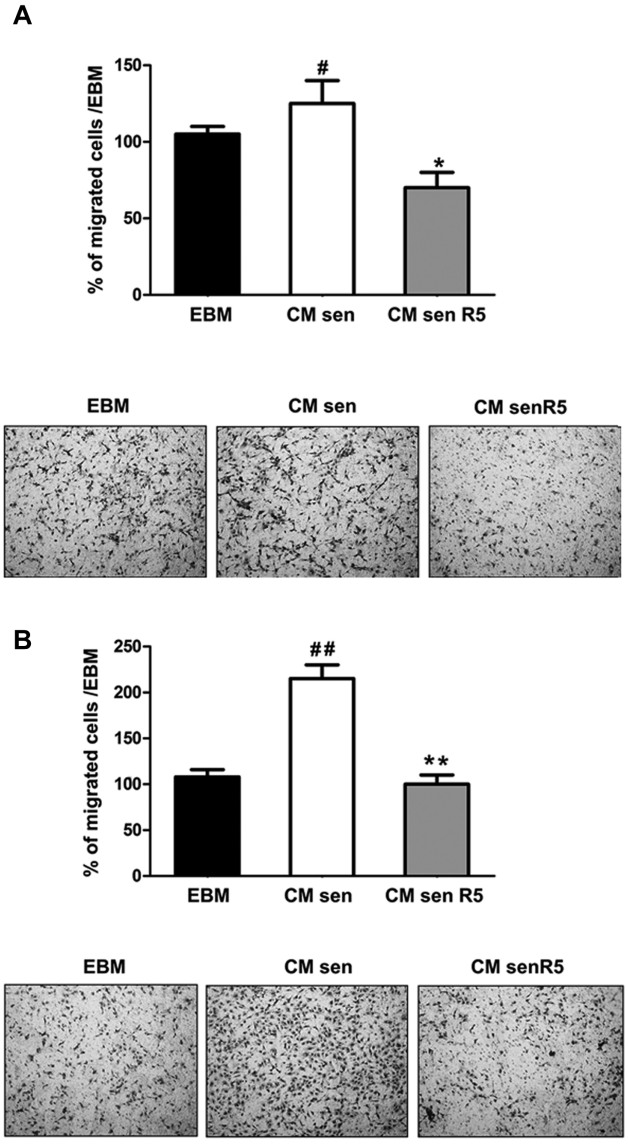

Figure 1. Effect of CM from MRC5 fibroblasts on the invasive activity of endothelial colony-forming cells (ECFCs). Invasion experiments were carried out for 6 hours at 37°C. (**A**) Chemoinvasion experiments. ECFCs (2.5 × 10^4 cells) were placed in the upper well while CM sen or CM senR5 were placed in the lower. Fresh unconditioned EBM was used as reference. Data are reported as the percentage of migrated cells toward CM sen or CM senR5 compared to those migrated toward fresh EBM (assumed as value 100%). # shows statistical significance ($p < .05$), compared to unconditioned EBM; * shows statistical significance ($p < .05$), compared to CM sen. (**B**) Spontaneous invasion. ECFCs were incubated overnight with CM sen, CM senR5, or unconditioned EBM (reference). Then 2.5 × 10^4 cells were suspended in the same media of the overnight incubation and placed in the upper well. Fresh EBM was placed in the lower well. Data are reported as the percentage of migrated cells after preincubation with MRC5 CM compared to those migrated toward fresh EBM (assumed as value 100%). All histograms represent the mean of three different experiments ± *SD*. ## shows high statistical significance ($p < .01$) compared to unconditioned EBM. ** shows high statistical significance ($p < .01$) compared to CM sen. Representative microphotographs (×10) of migrated cells are shown under the respective histogram.

Statistical Analysis

Statistical analyses of the data were performed using one-way ANOVA, and $p \leq .05$ was considered a statistically significant difference whereas $p \leq .01$ a very significant difference.

Results

MRC5 Senescent Phenotype and Resveratrol Effects

The senescent phenotype of MRC5 fibroblasts and the effect of R5 treatment on these traits have been shown in Supplementary Figure 1. Pre-senescent MRC5 fibroblasts (PDL values around 45) were grown in culture for about 5 weeks with or without 5 μM final resveratrol concentration. Control- and resveratrol-treated MRC5 cultures were referred to as sen and senR5. Growth curves (Supplementary Figure 1A) show very similar trend in both culture conditions, with a little increment of growth rate in R5-treated cells after the first week (around 10 days) of treatment. R5 treatment was not effective in overcoming the senescent replicative blockage, which was attained around PDL 55 in both cultures.

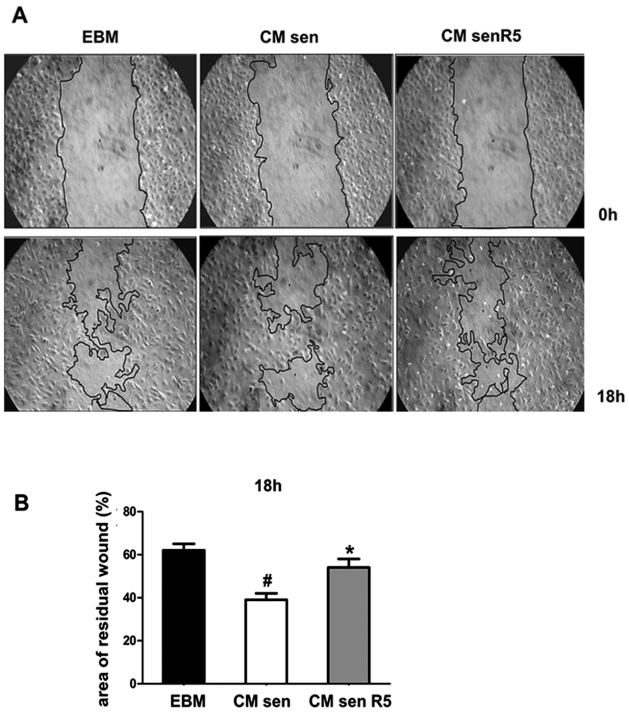

Figure 2. Effect of CM from MRC5 fibroblasts on wound healing of endothelial colony-forming cells (ECFCs). Conditioned media from senescent cultures, either untreated (CM sen) or treated for 5 weeks with resveratrol (CM senR5), were used in wound-healing assay of ECFCs. (**A**) Representative microphotographs (×10) at 0 and 18 hours from the wound are shown. (**B**) Histograms represent the percentage of the residual wound area (the mean of three different experiments ± *SD* is reported) measured after incubation with CM sen or CM senR5 compared to fresh EBM. # shows statistical significance ($p < .05$) compared to unconditioned EBM. * shows statistical significance ($p < .05$) compared to CM sen.

Cell extracts were submitted to Western blot analyses to determine p16 protein content (Supplementary Figure 1B), which was found increased, as expected, with the progression of senescence in MRC5 fibroblasts. In particular, p16 protein level in sen cultures was 50% higher than in pre-senescent fibroblasts and almost double than in low PDL young cultures. R5 treatment was not capable to significantly reduce p16 expression in senescent cells. Senescence-associated β-galactosidase staining (Supplementary Figure 1C) increased in sen compared to pre-senescent fibroblasts, and significantly reduced in senR5 cultures. The presence and the effect of R5 treatment on MRC5 apoptosis during our experimental protocol was evaluated by TUNEL assay in young, sen and senR5 cultures (Supplementary Figure 2). No apoptotic cells were detected in all experimental conditions, whereas DNAse I–treated sen fibroblasts, used as positive control, gave the green apoptotic signal. These experiments also allowed to appreciate nuclear enlargement in DAPI-stained sen MRC5 cells (17), another feature of replicative senescence.

Effect of MRC5 CMs on the Angiogenic Properties of ECFCs

ECFC cultures were incubated overnight with different media, following the experimental design summarized in Supplementary Figure 1. Cells were then collected, counted, and used for subsequent analyses herein reported.

Chemoinvasion and spontaneous invasion experiments were carried out as described in the Materials and Methods section. After 6 hours incubation at 37°C, cells that had passed through the lower surface of the filters were photographed and counted. Histograms report the percentage of the cell counts, taking the control condition (EBM) as 100%. A representative set of microphotographs of cells that passed the filter is also shown (Figure 1). In chemioinvasion assay (Figure 1A), CM from senescent MRC5 cultures (CM sen) stimulated only slightly the invasion of ECFCs, with a 20% increase of migrated cells compared to unconditioned EBM. Conversely, CM from senR5 fibroblasts (CM senR5) reduced the invasiveness of ECFCs of more than 50% compared to CM sen, attaining values even lower than untreated control ECFCs. In spontaneous invasion experiments (Figure 1B), ECFCs were incubated overnight with different conditioned media and then collected, counted, and seeded in the upper chamber of Matrigel-coated transwells as described earlier, with standard EBM plus 2% FBS in all lower chambers. Cells pretreated with CM sen showed a strong increase in spontaneous invasive activity compared to unconditioned EBM (+110%), whereas it was brought back to basal levels in cells pretreated with CM senR5.

Cell migration activity was also assayed with the wound-healing test (Figure 2). The analyses of the wells 18 hours after the wound clearly showed that CM senR5 reduced the CM sen–induced increase in cell migration, compared to unconditioned medium. Histograms report the quantification of the residual wound area, showing about 30% reduction of ECFC motility upon CM senR5 treatment compared to CM sen.

To evaluate the effects of the different conditioned media on the ability of ECFCs to form new blood vessels, a capillary morphogenesis test on Matrigel was employed as described in the Materials and Methods (Figure 3). When suspended in CM sen, the cells exhibited a much higher ability to form new tubes and networks compared to those in unconditioned EBM, as shown by an increased number

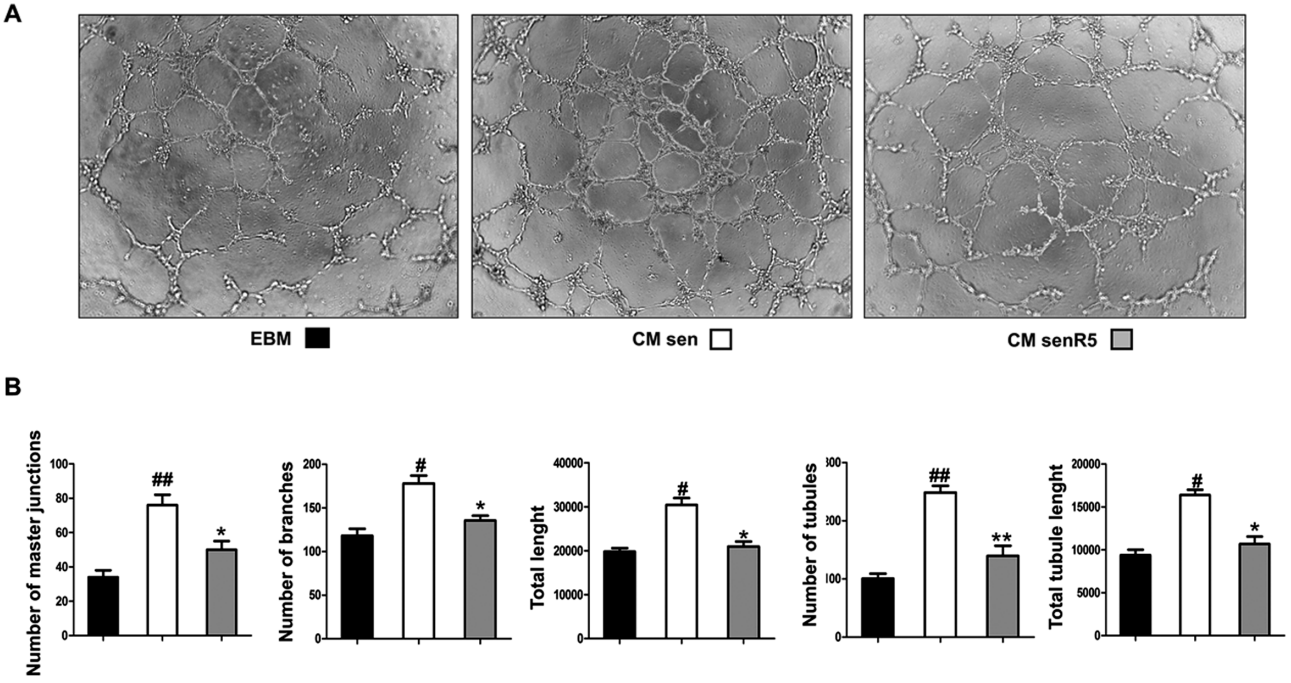

Figure 3. Effect of CM from MRC5 fibroblasts on capillary morphogenesis of endothelial colony-forming cells (ECFCs). ECFCs were incubated overnight with CM sen or CM senR5 or EBM used as reference medium. Then, cells were suspended in the same media of the overnight incubation and capillary morphogenesis assays were performed for 6 hours at 37°C. (**A**). Representative microphotographs (×10) of capillary-like structures are shown after incubation with CM sen, CM senR5, and EBM. (**B**) Quantification of capillary network of ECFCs by Angiogenesis Analyzer Image J tool. Histograms represent the mean number of master junctions, branches, tubules, total length, and total tubule length, respectively. Data are representative of measures obtained from six to nine fields. # shows statistical significance ($p < .05$); ## shows high statistical significance ($p < .01$), compared to unconditioned EBM. * shows statistical significance ($p < .05$); ** shows high statistical significance ($p < .01$), compared to CM sen.

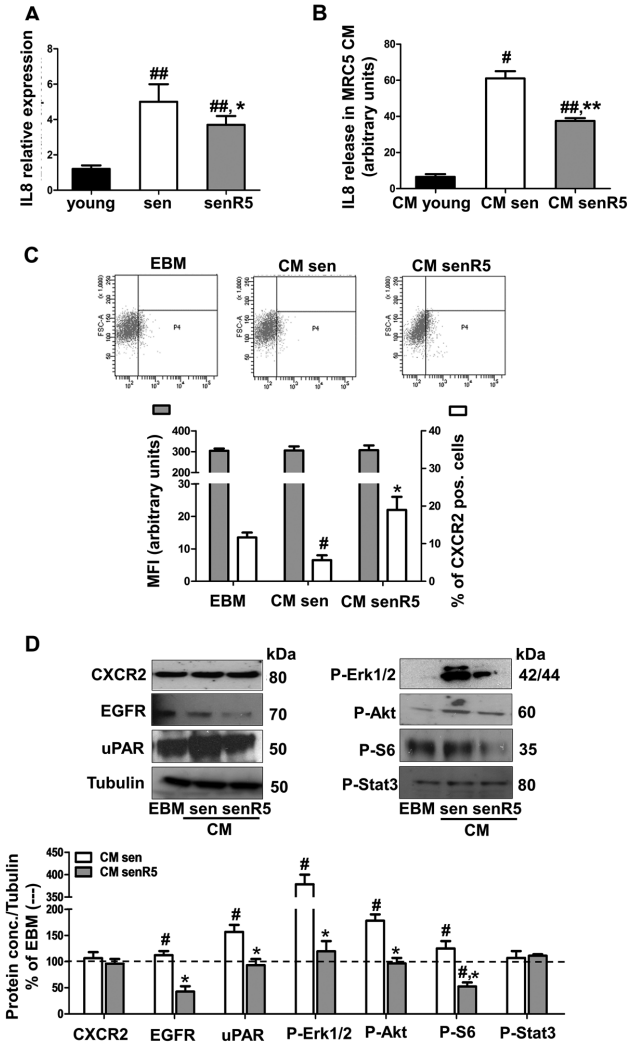

Figure 4. IL8 expression and release in MRC5 fibroblasts and effect of CM on receptor profile and IL8-dependent signaling pathways in endothelial colony-forming cells (ECFCs). (**A**) MRC5 pre-senescent fibroblasts were treated for 5 weeks with 5 μM resveratrol (senR5), or with standard medium (sen) until senescence; untreated low population doubling level cells were also assayed (young). At the end of the treatment, cells were analyzed for the expression of IL8 by Real Time PCR, using 18S rRNA as housekeeping gene. Histogram represents values normalized to young cultures (assumed as value 1) according to $2-\Delta\Delta Ct2-\Delta\Delta Ct$ method. ## shows high statistical significance ($p < .01$), compared to young values. * shows statistical significance ($p < .05$) compared to sen values. (**B**) The 24 hour conditioned media were collected from untreated (CM sen), R5-treated (CM senR5), and young cultures (CM young). IL-8 levels were measured by an ELISA. All the data are the mean of three different experiments ± *SD*. # shows statistical significance ($p < .05$); ## shows high statistical significance ($p < .01$), compared to young values. ** shows high statistical significance ($p < .01$), compared to sen values. (**C**) ECFCs were incubated overnight with CM sen or CM senR5 or EBM used as reference medium and then analyzed for CXCR2 expression by flow cytometry. Representative FACS dot plots are shown on the top. Histograms (on the bottom) represent the mean of % positive cells and the mean of fluorescence intensity (MFI). # shows statistical significance ($p < .05$) compared to unconditioned EBM. * shows statistical significance ($p < .05$) compared to CM sen. (**D**). Western blotting analysis of CXCR2, EGFR, uPAR, and of P-Erk1/2, P-Akt, P-S6, and P-Stat3 in ECFCs after overnight incubation with CM sen, CM senR5, or unconditioned EBM. Tubulin was used as a loading control. Bands were quantified by Image J. Results, reported as percentage, were normalized to values obtained after incubation with unconditioned EBM (assumed as value 100%, dot line). All histograms represent the mean of three different experiments ± *SD*. # shows statistical significance ($p < .05$) compared to unconditioned EBM. * shows statistical significance ($p < .05$) compared to CM sen.

of master junctions, branches, and tubules and by tubule and total length (Figure 3B), whereas cells suspended in CM senR5 showed only a modest increase of capillary forming activity. For example, the number of tubules resulted more than doubled in CM sen incubation, and were brought back to levels only slightly higher than control in CM senR5-incubated cells.

IL8 Expression and Release in Conditioned Media After Chronic Resveratrol Treatment of MRC5 Fibroblasts

Senescent control (sen) and resveratrol-treated (senR5) MRC5 cultures, along with low PDL fibroblasts (young), were analyzed for the expression and secretion of IL8 cytokine in conditioned media (Figure 4). Both gene expression (Figure 4A) and levels of IL8 in CM (Figure 4B) were increased in senescent MRC5 cells compared to young cells, as expected (18), attaining levels about five and six time higher, respectively. R5 treatment was capable to significantly lower both cytokine mRNA and its release in the medium (30% and 36%, respectively), compared to untreated senescent fibroblasts.

Effect of MRC5 CM on ECFC Receptor Profile and Intracellular Signaling Pathways

In these experiments, ECFC cultures were treated overnight with the described MRC5 CM. After incubation, cells were collected, and used to analyze CXCR2 expression by flow cytometry and to obtain cell protein extracts (Figure 4). Figure 4C shows the results of FACS analysis on CXCR2 expression: the percentage of CXCR2-positive cells was significantly lowered in ECFCs treated with CM sen compared with EBM incubation, and this change was completely reverted in CM senR5-treated cells. Moreover, the mean of fluorescence intensity was the same in all three conditions. The results of Western blot analysis (Figure 4D) confirmed no difference in CXCR2 protein levels, thus suggesting a reduced CXCR2 expression at membrane level in CM sen–treated ECFCs compared to both CM senR5–treated and untreated ECFCs.

CM sen induced a significant increase of uPAR protein content in ECFCs, compared to unconditioned EBM, whereas EGFR was similarly expressed. However, cells treated with CM senR5 showed a much lower expression of both receptors, as compared to CM sen. As for intracellular kinase signaling pathways, the incubation with CM sen induced a strong increase of both phosphorylated ERK proteins compared to EBM, attaining about a fourfold total amount, and about a 60% increase of P-Akt, whereas the phosphorylation of S6 and Stat3 resulted to be only slightly or not modified. The treatment with CM senR5 heavily reduced intracellular phosphorylation pathways: P-ERK was found fivefold less than with CM sen, and P-Akt was brought down to levels similar to control EBM condition. CM senR5 treatment also reduced P-S6 to levels about 50% of untreated ECFCs, whereas Stat3 phosphorylation was unaffected by all CM incubations.

Effects of IL8-Depletion on the Pro-angiogenic Trait of CM sen

To verify to which extent the stimulation of capillary morphogenesis by CM sen was due to IL8 signaling, in some experiments ECFCs were exposed to CM sen depleted of IL8, as described in the Materials and Methods. Figure 5A shows the results of IL8 immunodetection in CM sen before and after IL8 depletion. Almost 90% of the cytokine was found to be removed, thus confirming the effectiveness of the

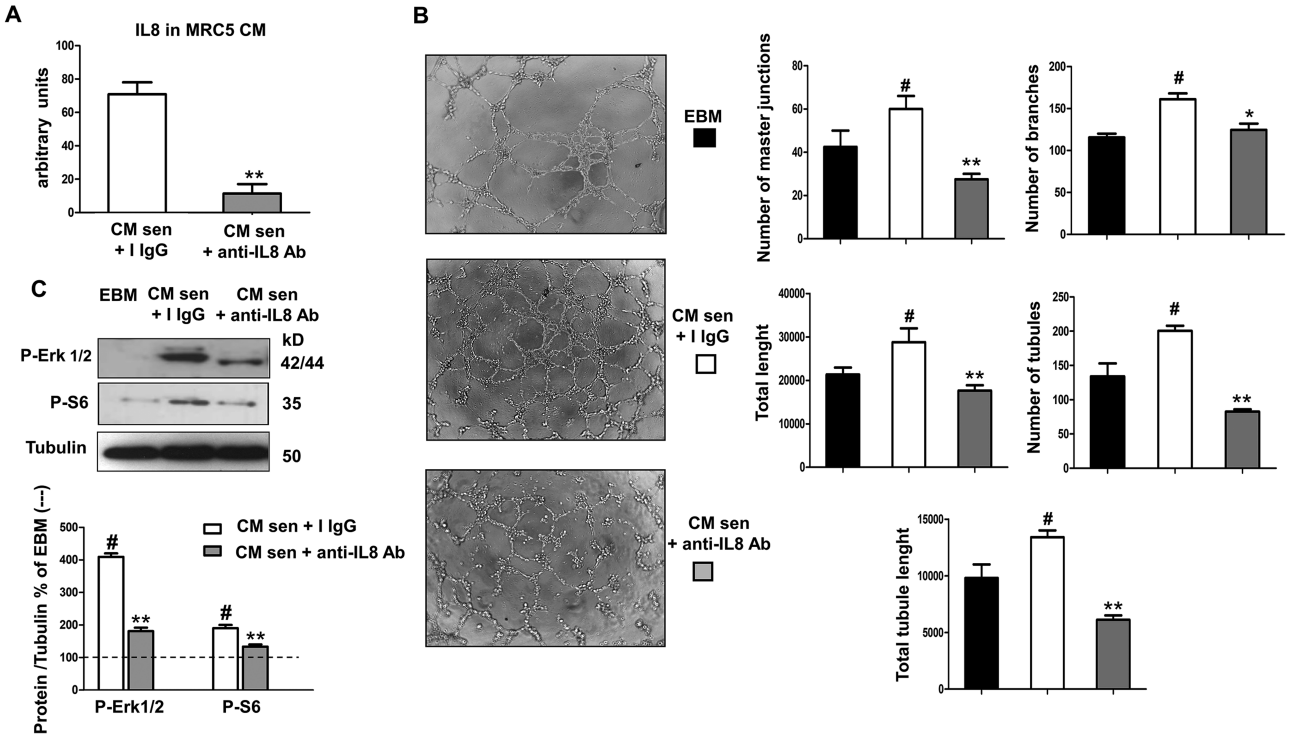

Figure 5. Effects of IL8-depletion on the pro-angiogenic trait of CM sen. CM sen was depleted of IL8 by means of Dynabeads Protein G after anti-IL8 antibody incubation. (**A**) ELISA assay was performed on IL8-depleted CM sen (CM sen + anti-IL8 Ab) and CM sen (CM sen + I IgG). Histograms represent the mean ± *SD* of three different determinations. ** shows high statistical significance ($p < .01$), compared to CM sen + I IgG. (**B**) Endothelial colony-forming cells (ECFCs) were incubated overnight with CM sen + I IgG, CM sen + anti-IL8 Ab or EBM used as reference medium. Then, cells were suspended in the same media of the overnight incubation and capillary morphogenesis assays were performed for 6 hours. Representative photographs (×10) of capillary-like structures are shown on the left. Quantification of ECFCs capillary network (on the right) was carried out by Angiogenesis Analyzer Image J tool. Histograms represent the mean number of master junctions, branches, tubules, total length, and total tubule length, respectively. Data are representative of measures obtained from six to nine fields (mean ± *SD*). # shows statistical significance ($p < .05$) compared to unconditioned EBM. * shows statistical significance ($p < .05$); ** shows high statistical significance ($p < .01$), compared to CM sen + I IgG. (**C**) Western blotting of ECFC extracts for P-Erk 1/2 and P-S6 levels after overnight incubation with CM sen + I IgG, CM sen + anti-IL8 Ab, or EBM. Tubulin was used as a loading control. Histograms represent the mean of three different experiments ± *SD*. Results, reported as percentage, were normalized to values obtained after incubation with unconditioned EBM (assumed as value 100%, dot line.) # shows statistical significance ($p < .05$) compared to unconditioned EBM. ** shows high statistical significance ($p < .01$), compared to CM sen + I IgG.

subtraction procedure. Indeed, the IL8-depleted CM sen (CM sen + anti-IL8 Ab) induced much less new capillary formation compared to the nondepleted CM sen (CM sen + I IgG) (Figure 5B), attaining values near or lower than those found in EBM-treated cultures, as shown by the number of master junctions, branches, and tubules and by tubule and total length. In parallel, Western blotting analyses (Figure 5C) on cell lysates of ECFCs treated with CM sen + I IgG or with CM sen + anti-IL8 Ab showed that the depletion of IL8 almost completely abrogated the CM sen increment in phosphorylation of both ERK and S6 proteins.

Discussion

The inhibition of the cross talk between stroma fibroblasts and cancer cells could be a potential target for future anticancer therapeutic efforts. Among the microenvironment factors, cell senescence plays a relevant role, both as a tumor-suppressing mechanism when cancer cells can be induced to senesce by chemotherapy (29) and as a tumor-promoting factor due to the complex secretory profile of senescent stroma components (30,31). Our data show that the SASP of senescent fibroblasts, and particularly IL8 secretion, has an essential role in enhancing the vasculogenic properties of tissue microenvironment.

Mechanisms that contribute to the formation of tumor-associated vasculature could serve as targets for designing new antiangiogenic therapies. ECFCs play an important role, especially in the early stages of tumor growth, when they are critical for promoting the "angiogenic switch," and during metastasis, when they promote the transition from micro- to macro-metastases (32).

Several natural agents, comprising resveratrol (33) have shown direct antiangiogenic effects in in vivo models of tumor angiogenesis. We previously reported that R5 chronic treatment induced a significant reduction of several SASP factors in senescent MRC5 fibroblasts (17,18), along with the inhibition of SASP pro-tumoral effects on melanoma cells (19). In this work, we confirmed the previously described (17) expression of a senescent phenotype in our model and its modulation by R5 treatment, that was effective in lowering senescence-associated β-galactosidase staining, without increasing the proliferative potential of senescent MRC5 fibroblasts. In addition, these senescent cells did not show apoptotic markers, even after R5 treatment.

Here we studied the effect of resveratrol-mediated modulation of senescent microenvironment on ECFCs, and showed an indirect antiangiogenic effect of R5 treatment, mediated by the modulation of MRC5 SASP. Among the several SASP factors lowered by R5 treatment of senescent MRC5 fibroblasts (18), here we focused on the role of IL8.

IL8 is the most abundant angiogenic cytokine produced by senescent fibroblasts (18), and is reported to be highly upregulated in

fibroblast-tumor cell cocultures (34). In this work, we confirmed an increase in IL8 gene expression by MRC5 fibroblasts upon senescence, followed by a higher level of the cytokine in the conditioned media (18) compared to young cells. Furthermore, we showed that CM sen was effective in enhancing the angiogenic properties of ECFCs. Functional assays revealed an enhancement of the invasive properties of ECFCs, in comparison with unconditioned medium, both when CM sen was used as chemoattractant, and when it was used in overnight preincubation of ECFCs before the invasion test, giving an even more pronounced effect in the latter case. In addition, ECFC motility augmented in wound-healing experiments upon CM sen incubation, with a parallel increase of capillary morphogenesis capability. All these features were reduced when ECFCs were exposed to media collected from R5 pretreated senescent MRC5 (CM senR5).

The expression of IL8–CXCR2 in the tumor microenvironment has been reported to have a pleiotropic role, with a limiting function mediated by senescence reinforcement in preneoplastic lesions, and with pro-tumorigenic effects in more advanced cancer stages (35). It plays a critical role in colon cancer (36) and has been indicated as one potential therapeutic target in prostatic cancer (37). We thus analyzed the expression of CXCR2, the cytokine receptor with the highest affinity for IL8 (38). Flow cytometry showed a SASP-dependent decrease of CXCR2-expressing cell number, without a parallel change in the amount and expression intensity of the receptor protein. This indicates that the IL8–CXCR2 interaction, with consequent receptor internalization (39), was enhanced in ECFCs exposed to senescent medium containing increased IL8 levels, as expected. On the contrary, in ECFCs incubated with CM senR5, CXCR2-positive cells were found increased, indicating that receptor internalization was reduced to levels even lower than in control EBM incubated cells.

ECFC phenotypic changes upon conditioned media exposure were also explained by the effects on EGFR and uPAR protein levels and on the related receptor-tyrosine-kinase signaling pathways (ERK, AKT/mTOR) (40,41), all enhanced by CM sen and reduced or abolished when ECFCs were exposed to CM senR5.

Finally, to verify the importance of IL-8 signaling in the observed effects, ECFCs were incubated with CM sen depleted of this cytokine, and the effect on both tubular morphogenesis and intracellular signaling resulted to be similar to that obtained with CM senR5. These data confirm a dominant role of IL8 in the modulation of the angiogenic properties of tissue microenvironment. Furthermore, they indicate that IL8 reduction is one of the main mechanisms through which resveratrol acts as an indirect modulator of angiogenesis. However, as resveratrol also reduces the release of other SASP factors (18,19), many of which have been reported to play a role in the modulation of the angiogenic phenotype of ECFCs (42), additional beneficial effects can derive from its ability to modify the SASP balance in a complex manner.

Resveratrol has the potential to attenuate many age-related chronic diseases and to improve overall health, by means of both its intrinsic antioxidant capacity and the activation/repression of a wide range of membrane receptors, kinases, and other enzymes (43). It is probably the combination of many different biological activities that ultimately leads to resveratrol health benefits. Among these, the ability of mitigating the SASP, particularly reducing IL8 levels, in tissue microenvironment appears to be a mean to lower the pro-angiogenic activity of stroma senescent cells, thus indirectly targeting cancer promotion.

Supplementary Material

Supplementary data are available at *The Journals of Gerontology, Series A: Biological Sciences and Medical Sciences* online.

Funding

This work was supported by funds from the University of Florence and from Associazione Italiana per la Ricerca sul Cancro to M.D.R. (AIRC, IG 2013 N.14266). Dr. Francesca Margheri was supported by postdoctoral fellowship of Fondazione Umberto Veronesi.

Conflict of Interest Statement

None declared.

References

1. Coppé JP, Patil CK, Rodier F, et al. Senescence-associated secretory phenotypes reveal cell-nonautonomous functions of oncogenic RAS and the p53 tumor suppressor. *PLoS Biol*. 2008;6:2853–2868. doi:10.1371/journal.pbio.0060301.
2. Davalos AR, Coppe JP, Campisi J, Desprez PY. Senescent cells as a source of inflammatory factors for tumor progression. *Cancer Metastasis Rev*. 2010;29:273–283. doi:10.1007/s10555-010-9220-9.
3. Campisi J. Aging, cellular senescence, and cancer. *Annu Rev Physiol*. 2013;75:685–705. doi:10.1146/annurev-physiol-030212-183653.
4. Xing F, Saidou J, Watabe K. Cancer associated fibroblasts (CAFs) in tumor microenvironment. *Front Biosci (Landmark Ed)*. 2010;15:166–179. doi:10.2741/3613.
5. Sitohy B, Nagy JA, Dvorak HF. Anti-VEGF/VEGFR therapy for cancer: reassessing the target. *Cancer Res*. 2012;72:1909–1914. doi:10.1158/0008-5472.CAN-11-3406.
6. Krtolica A, Parrinello S, Lockett S, Desprez PY, Campisi J. Senescent fibroblasts promote epithelial cell growth and tumorigenesis: a link between cancer and aging. *Proc Natl Acad Sci USA*. 2001;98:12072–12077. doi:10.1073/pnas.211053698.
7. Acosta JC, O'Loghlen A, Banito A, Raguz S, Gil J. Control of senescence by CXCR2 and its ligands. *Cell Cycle*. 2008;7:2956–2959. doi:10.4161/cc.7.19.6780.
8. Hampel B, Fortschegger K, Ressler S, et al. Increased expression of extracellular proteins as a hallmark of human endothelial cell in vitro senescence. *Exp Gerontol*. 2006;41:474–481. doi:10.1016/j.exger.2006.03.001.
9. Végran F, Boidot R, Michiels C, Sonveaux P, Feron O. Lactate influx through the endothelial cell monocarboxylate transporter MCT1 supports an NF-κB/IL-8 pathway that drives tumor angiogenesis. *Cancer Res*. 2011;71:2550–2560. doi:10.1158/0008-5472.CAN-10-2828.
10. Li A, Dubey S, Varney ML, Dave BJ, Singh RK. IL-8 directly enhanced endothelial cell survival, proliferation, and matrix metalloproteinases production and regulated angiogenesis. *J Immunol*. 2003;170:3369–3376. doi:10.4049/jimmunol.170.6.3369.
11. Ortiz-Montero P, Londoño-Vallejo A, Vernot JP. Senescence-associated IL-6 and IL-8 cytokines induce a self- and cross-reinforced senescence/inflammatory milieu strengthening tumorigenic capabilities in the MCF-7 breast cancer cell line. *Cell Commun Signal*. 2017;15:17. doi:10.1186/s12964-017-0172-3.
12. Cao Z, Shang B, Zhang G, et al. Tumor cell-mediated neovascularization and lymphangiogenesis contrive tumor progression and cancer metastasis. *Biochim Biophys Acta*. 2013;1836:273–286. doi:10.1016/j.bbcan.2013.08.001.
13. Liu J, Huang J, Yao WY, et al. The origins of vacularization in tumors. *Front Biosci (Landmark Ed)*. 2012;17:2559–2565.
14. Pitozzi V, Jacomelli M, Catelan D, et al. Long-term dietary extra-virgin olive oil rich in polyphenols reverses age-related dysfunctions in motor coordination and contextual memory in mice: role of oxidative stress. *Rejuvenation Res*. 2012;15:601–612. doi:10.1089/rej.2012.1346.

15. Pearson KJ, Baur JA, Lewis KN, et al. Resveratrol delays age-related deterioration and mimics transcriptional aspects of dietary restriction without extending life span. *Cell Metab*. 2008;8:157–168. doi:10.1016/j.cmet.2008.06.011.
16. Muhammad MH, Allam MM. Resveratrol and/or exercise training counteract aging-associated decline of physical endurance in aged mice; targeting mitochondrial biogenesis and function. *J Physiol Sci*. 2018;68:681–688. doi:10.1007/s12576-017-0582-4.
17. Giovannelli L, Pitozzi V, Jacomelli M, et al. Protective effects of resveratrol against senescence-associated changes in cultured human fibroblasts. *J Gerontol A Biol Sci Med Sci*. 2011;66:9–18. doi:10.1093/gerona/glq161.
18. Pitozzi V, Mocali A, Laurenzana A, et al. Chronic resveratrol treatment ameliorates cell adhesion and mitigates the inflammatory phenotype in senescent human fibroblasts. *J Gerontol A Biol Sci Med Sci*. 2013;68:371–381. doi:10.1093/gerona/gls183.
19. Menicacci B, Laurenzana A, Chillà A, et al. Chronic resveratrol treatment inhibits MRC5 fibroblast SASP-related protumoral effects on melanoma cells. *J Gerontol A Biol Sci Med Sci*. 2017;72:1187–1195. doi:10.1093/gerona/glw336.
20. Kim CW, Hwang KA, Choi KC. Anti-metastatic potential of resveratrol and its metabolites by the inhibition of epithelial-mesenchymal transition, migration, and invasion of malignant cancer cells. *Phytomedicine*. 2016;23:1787–1796. doi:10.1016/j.phymed.2016.10.016.
21. Varoni EM, Lo Faro AF, Sharifi-Rad J, Iriti M. Anticancer molecular mechanisms of resveratrol. *Front Nutr*. 2016;3:8. doi:10.3389/fnut.2016.00008.
22. Samadi AK, Bilsland A, Georgakilas AG, et al. A multi-targeted approach to suppress tumor-promoting inflammation. *Semin Cancer Biol*. 2015;35 (suppl):S151–S184. doi:10.1016/j.semcancer.2015.03.006.
23. Shanmugam MK, Warrier S, Kumar AP, Sethi G, Arfuso F. Potential role of natural compounds as anti-angiogenic agents in cancer. *Curr Vasc Pharmacol*. 2017;15:503–519. doi:10.2174/1570161115666170713094319.
24. Radomska-Leśniewska DM, Bałan BJ, Skopiński P, et al. Angiogenesis modulation by exogenous antioxidants. *Cent Eur J Immunol*. 2017;42:370–376. doi:10.5114/ceji.2017.72804.
25. Elkhattouti A, Hassan M, Gomez CR. Stromal fibroblast in age-related cancer: role in tumorigenesis and potential as novel therapeutic target. *Front Oncol*. 2015;5:158. doi:10.3389/fonc.2015.00158.
26. Margheri F, Chillà A, Laurenzana A, et al. Endothelial progenitor cell-dependent angiogenesis requires localization of the full-length form of uPAR in caveolae. *Blood*. 2011;118:3743–3755. doi:10.1182/blood-2011-02-338681.
27. Menicacci B, Cipriani C, Margheri F, Mocali A, Giovannelli L. Modulation of the senescence-associated inflammatory phenotype in human fibroblasts by Olive Phenols. *Int J Mol Sci*. 2017;18:2275. doi:10.3390/ijms18112275.
28. Margheri F, Serratì S, Lapucci A, et al. Modulation of the angiogenic phenotype of normal and systemic sclerosis endothelial cells by gain-loss of function of pentraxin 3 and matrix metalloproteinase 12. *Arthritis Rheum*. 2010;62:2488–2498. doi:10.1002/art.27522.
29. Rao SG, Jackson JG. SASP: tumor suppressor or promoter? Yes! *Trends Cancer*. 2016;2:676–687. doi:10.1016/j.trecan.2016.10.001.
30. Lecot P, Alimirah F, Desprez PY, Campisi J, Wiley C. Context-dependent effects of cellular senescence in cancer development. *Br J Cancer*. 2016;114:1180–1184. doi:10.1038/bjc.2016.115.
31. Coppé JP, Desprez PY, Krtolica A, Campisi J. The senescence-associated secretory phenotype: the dark side of tumor suppression. *Annu Rev Pathol*. 2010;5:99–118. doi:10.1146/annurev-pathol-121808-102144.
32. Moschetta M, Mishima Y, Sahin I, et al. Role of endothelial progenitor cells in cancer progression. *Biochim Biophys Acta*. 2014;1846:26–39. doi:10.1016/j.bbcan.2014.03.005.
33. Kumar M, Dhatwalia SK, Dhawan DK. Role of angiogenic factors of herbal origin in regulation of molecular pathways that control tumor angiogenesis. *Tumour Biol*. 2016;37:14341–14354. doi:10.1007/s13277-016-5330-5.
34. Tan PH, Chia SS, Toh SL, Goh JC, Nathan SS. The dominant role of IL-8 as an angiogenic driver in a three-dimensional physiological tumor construct for drug testing. *Tissue Eng Part A*. 2014;20:1758–1766. doi:10.1089/ten.TEA.2013.0245.
35. Acosta JC, Gil J. A role for CXCR2 in senescence, but what about in cancer? *Cancer Res*. 2009;69:2167–2170. doi:10.1158/0008-5472.CAN-08-3772.
36. Lee YS, Choi I, Ning Y, et al. Interleukin-8 and its receptor CXCR2 in the tumour microenvironment promote colon cancer growth, progression and metastasis. *Br J Cancer*. 2012;106:1833–1841. doi:10.1038/bjc.2012.177.
37. Maxwell PJ, Neisen J, Messenger J, Waugh DJ. Tumor-derived CXCL8 signaling augments stroma-derived CCL2-promoted proliferation and CXCL12-mediated invasion of PTEN-deficient prostate cancer cells. *Oncotarget*. 2014;5:4895–4908. doi:10.18632/oncotarget.2052.
38. Chuntharapai A, Kim KJ. Regulation of the expression of IL-8 receptor A/B by IL-8: possible functions of each receptor. *J Immunol*. 1995;155:2587–2594. ISSN: 0022-1767.
39. Ha H, Debnath B, Neamati N. Role of the CXCL8-CXCR1/2 axis in cancer and inflammatory diseases. *Theranostics*. 2017;7:1543–1588. doi:10.7150/thno.15625.
40. Laurenzana A, Chillà A, Luciani C, et al. uPA/uPAR system activation drives a glycolytic phenotype in melanoma cells. *Int J Cancer*. 2017;141:1190–1200. doi:10.1002/ijc.30817.
41. Binder BR, Mihaly J, Prager GW. uPAR-uPA-PAI-1 interactions and signaling: a vascular biologist's view. *Thromb Haemost*. 2007;97:336–342. doi:10.1160/TH06–11–0669.
42. Oubaha M, Miloudi K, Dejda A, et al. Senescence-associated secretory phenotype contributes to pathological angiogenesis in retinopathy. *Sci Transl Med*. 2016;8:362ra144. doi:10.1126/scitranslmed.aaf9440.
43. Kulkarni SS, Cantó C. The molecular targets of resveratrol. *Biochim Biophys Acta*. 2015;1852:1114–1123. doi:10.1016/j.bbadis.2014.10.005.